Fast and reliable storage using a 5-bit, non-volatile photonic memory cell: supplementary material

Xuan Li[1], Nathan Youngblood[1], Carlos Ríos[1,2], Zengguang Cheng[1], C. David Wright[3],Wolfram HP Pernice[4], and Harish Bhaskaran[1,*]

[1]*Department of Materials, University of Oxford, UK*
[2]*Present address: Department of Materials Science & Engineering, Massachusetts Institute of Technology, USA*
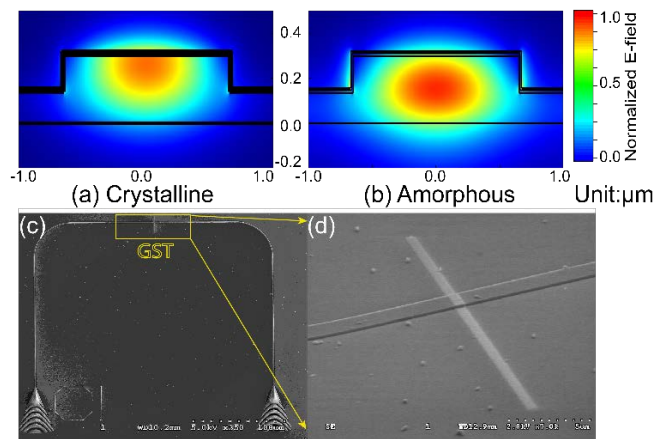[3]*Department of Engineering, University of Exeter, UK*
[4]*Department of Physics, University of Münster, Germany*

Corresponding author: harish.bhaskaran@materials.ox.ac.uk

This document provides supplementary information to "Fast and reliable storage using a 5-bit, non-volatile photonic memory cell," https://doi.org/10.1364/OPTICA.6.000001. This supplementary document includes simulation results, the optical setup details and the arbitrary modulation of single pulse programming with variation of the amplitude of 2nd step.
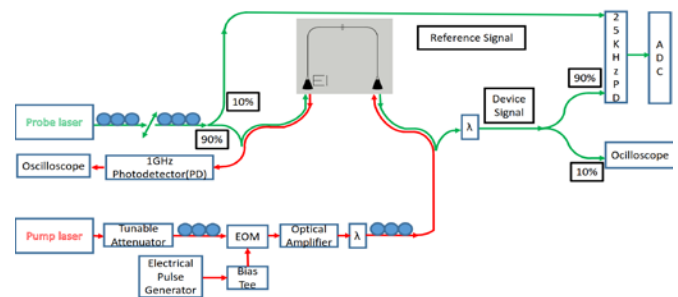
Figure S1 simulation of different states and SEM image of one phase change photonic memory device. (a) Light propagation TE mode with crystalline GST. (b) Light propagation TE mode with amorphous GST. (c) SEM image of the whole phase change photonic device. (d) Zoom-in SEM image of GST.

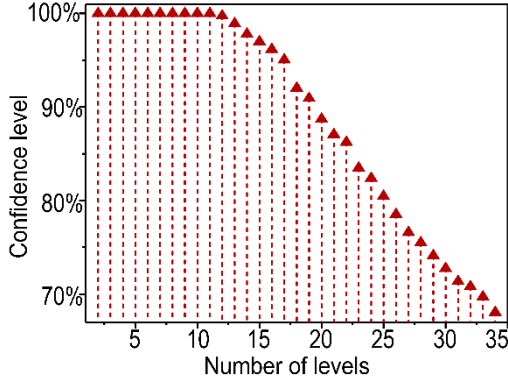**Simulation of light propagation under different states of GST.** Figure S1 (a) and (b) show FDE Mode simulation results of light propagation modes with crystalline GST or amorphous GST through the waveguide. Figure S1 (c), (d) shows the geometry of GST material on the top of the waveguide. It can be illustrated from the Figure S1 simulation that when the phase of GST changes from crystalline to amorphous which can be tuned by increasing power, light propagation changes a lot. And its ability of light absorption changes as well. With increasing power, the area of amorphous GST becomes larger (Figure 1(c)) and the transmission become higher. We use refractive indices of different materials from [1].

Measurement setup. The schematic of optical setup we use for measurement is shown in Figure S2. There are two optical circuits (red lines and green lines) for level addressing and monitoring separately. The probe light (green line) generates from probe laser, go through two polarization controller paddles and an in-line polarizer to fix the polarization. Subsequently after one beam splitter, 10% power directly go to photodetector as a reference
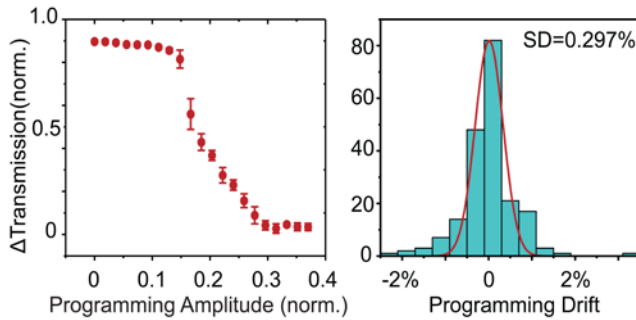

Figure S2 Schematic of measurement setup.

signal to remove potential environment noise and drifts, 90% power go through the device to detect the state of the device. The probe signal is reduced to 0.1mW to reduce potential drifts caused by thermos-optical effect of GST. However, more precise and repeatable multilevels can be achieved with lower noise and higher signal resolution of the photodetector. The power of the pump light (red line) is modulated by EOM controlled by an electrical pulse generator via a bias tee to generate nanosecond light pulses. These two routes are separated by circulators and optical filters.

Figure S3 Here we plot the confidence level (non-overlapping levels from statistical data from Figure 2c in the main text) as a function of the number of equally separated transmission levels. Our results show that for 32 levels, we can reach an arbitrary transmission level using a single programming pulse with a confidence of 71%.

Repeatability of deterministically reaching levels with a single ERASE/Programming pulse. In Figure 2(a) of the main text, we demonstrate that 34 individual levels can be easily resolved from each other once programmed. However, from Figure 2(b) of the main text, for multiple programming cycles we can see a non-negligible overlap in the error bars of neighboring levels. We attribute this to slight variations between programming pulses and optical readout due to environmental drift in our experimental setup. In order to quantify this variation, we plot the degree of confidence versus the number of non-overlapping levels we can achieve in our device (see Figure S3). As we add more levels, our confidence in arriving at a certain level without overlapping with a neighboring level decreases. We can see from Figure S3 that using a single pulse, we can achieve up to 11 levels with 100% accuracy, up to 19 levels with 90% accuracy, up to 26 levels with 80% accuracy, and up to 32 levels with an accuracy of 71%.

Figure S4 The final transmission state of GST for arbitrary programmed amplitude of the pulse's trailing end.

Arbitrary modulation programming with variation of the amplitude. We use labview programming to generate gradually or arbitrarily changeable pump pulses sent to devices. For the dual-pulse modulation, all the amplitude of pump pulses increases equally step by step in the gradual modulation. For the arbitrary modulation, we vary the parameter of both decay time (see Figure 4(c)) and decay amplitude. Figure S4 shows the transmission levels and deviation distribution and separate error bar distribution of different levels of random programming pulse

amplitude. The modulation of decay time shows much better linearity and stability.

REFERENCES

1. C. Rios, P. Hosseini, C. D. Wright, H. Bhaskaran, and W. H. P. Pernice, "On-chip photonic memory elements employing phase-change materials," Adv. Mater. **26**, 1372–1377 (2014).